Autonomous Monitoring of Fluid Movement Using 3-D Electrical Resistivity Tomography

Douglas J. LaBrecque[1], Gail Heath[2], Roger Sharpe[1] and Roelof Versteeg[2]
[1]Multi-Phase Technologies, LLC, Sparks Nev.
[2]Idaho National Engineering and Environmental Laboratory, Idaho Falls, Idaho.

ABSTRACT

The electrical resistivity tomography method (ERT) is seeing increasing use in long-term monitoring. Applications might include monitoring of advanced remediation methods, vadose zone fluid-flow monitoring, and monitoring below tanks at the Hanford reservation. For this method to be cost effective, future systems will need to be highly automated.

This paper compares different strategies for collecting three-dimensional (3-D) data sets. We discuss the critical design aspects of the system and the importance of using integrated hardware for data collection, and software for data interpretation.

An autonomous acquisition system was used to monitor a field experiment at the Idaho National Engineering and Environmental Laboratory. The system was successful at collecting data that were used to monitor infiltration of water into interbedded sediment and basalt layers. The results showed the advantages of autonomous systems for collecting data, and the need for robust operating systems designed specifically for autonomous operation.

Introduction

One of the most promising geophysical techniques, for remediation-process and long-term subsurface environmental monitoring, is electrical resistivity tomography (ERT). ERT is an adaptation of the traditional surface resistivity method. Whereas traditional resistivity surveys use a relatively small number of measurements collected along a single line using a single specific electrode pattern/array, ERT employs the collection of large, high-density data sets using two-dimensional (2-D) or three-dimensional (3-D) arrays of electrodes. Often a large number of the electrodes are emplaced in boreholes.

ERT has some unique qualities that make it amenable to environmental monitoring. The method is sensitive to fluid content, saturation, and composition, as well as subsurface temperature. ERT has a demonstrated ability to measure very small changes in subsurface properties over time. For these reasons the technique has seen increasing use for monitoring of new, aggressive, environmental remediation processes (Ramirez *et al.,* 1993, 1995; LaBrecque *et al.,* 1996b, 1997, 1998), leak detection (Daily and Ramirez, 1999), and monitoring of both saturated and vadose zone transport processes (Daily *et al.,* 1992; LaBrecque and Casale, 2002). The ERT method is an extension of the classic resistivity method but differs in that it typically uses a large number (often several hundreds) of electrodes placed both on the surface and within boreholes. Because the electrodes are simple and inexpensive, they are generally grouted permanently in place. These permanent installations create unique opportunities for both data collection and interpretation.

Previous work by LaBrecque and Yang (2001) describes an interpretation method that capitalizes on the ability of the method to make highly repeatable measurements. The goal of this paper is to discuss progress in developing data collection and processing strategies that promise to make ERT far more efficient and cost effective for long-term monitoring. An ideal, fully-automated system would collect, process and image ERT data with minimal human oversight. Although this holds the promise of making ERT much more cost effective for long-term monitoring applications, it creates unique challenges for overall system design and implementation.

Within this paper we discuss the development of a prototype to a fully-automated system and its application at a test site at the Idaho National Engineering and Environmental Laboratory (INEEL) in Southeastern Idaho.

Overview of ERT

The ERT method relies on sophisticated acquisition systems and modeling algorithms. The evolution of ERT has closely followed the development of fast, cheap computers. The first significant work on ERT began in the 1980′s. Notable work at this time was the 2-D modeling of Schima (Shima and Sakayama, 1987; Shima, 1990) that was based on the alpha-center method inverted using back-projection methods; and the 2-D finite-element modeling of Sasaki (Sasaki, 1992). Following the development of Occam's style

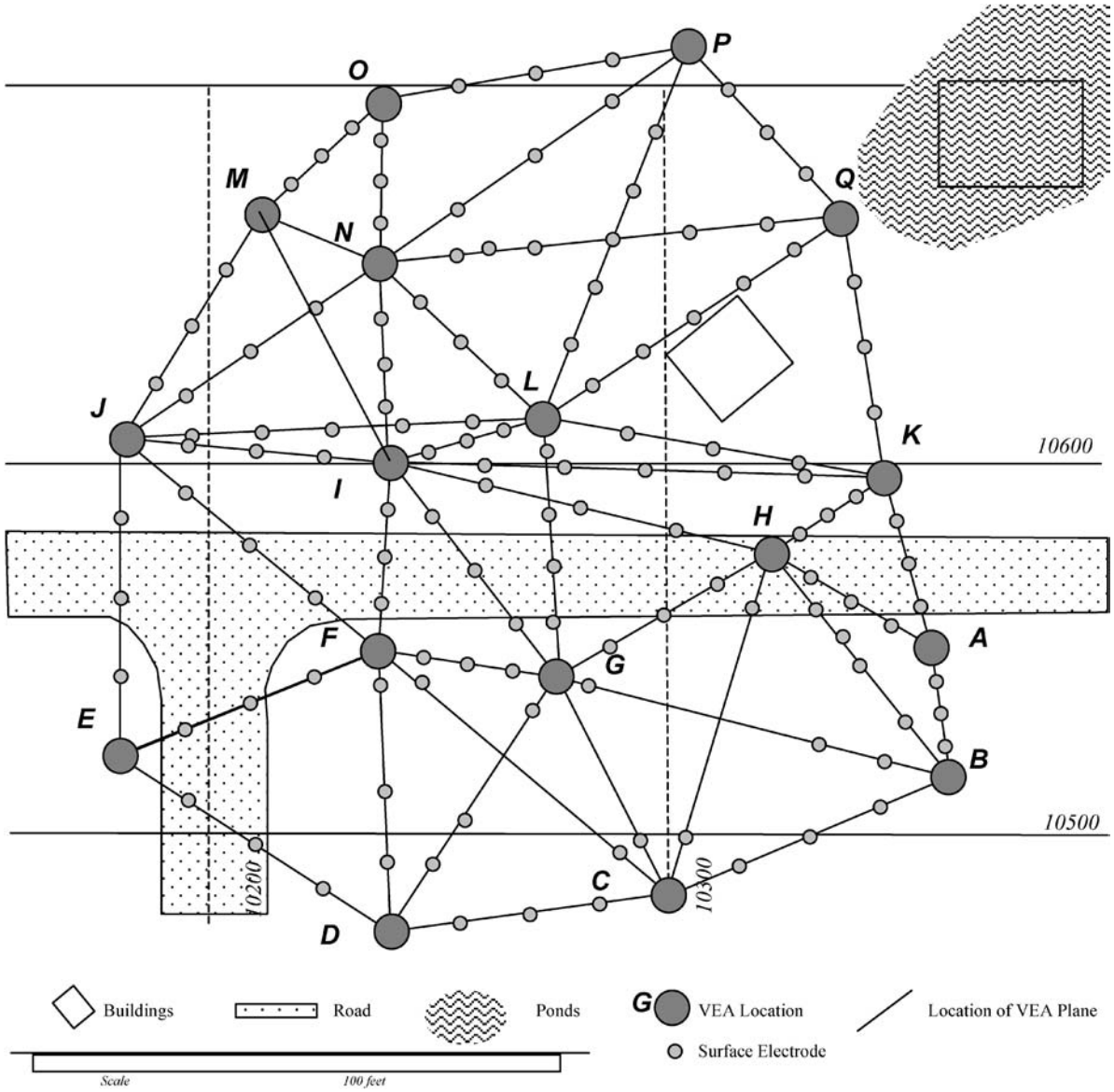

Figure 1. Example of the layout of VEA (large circles), surface electrodes (small circles) and data planes for ERT at the Portsmouth Gaseous Diffusion Plant.

inversion routines (LaBrecque *et al.,* 1996a), ERT was applied to a wide range of environmental and engineering problems. These included the monitoring of vadose zone water movement (Daily *et al.,* 1992; Schima *et al.,* 1993), steam injection (Ramirez *et al.,* 1993; LaBrecque *et al.,* 1998), and air sparging (Schima *et al.,* 1996; Lundegard and LaBrecque, 1995, 1998).

There have been continuous improvements in ERT interpretation over the last decade. These include the development of efficient 3-D routines (Sasaki, 1994; Zhang *et al.,* 1995; LaBrecque *et al.,* 1999), the development of a robust inversion scheme that allows for non-Gaussian distributed noise (Morelli and LaBrecque, 1996), and the modeling of metal well casings within the 3-D codes (LaBrecque *et al.,* 1998).

Data Collection Strategies

Two-Dimensional Data Collection Strategies

The use of ERT for monitoring of remediation on a large scale requires that very large data sets be processed and imaged in less than 24 hours. The images must be high quality and reliable. To understand both the advantages of, and the difficulties in organizing and processing fully 3-D data consider a typical, 2-D field layout and how it might be done in 3-D. Traditionally, all of the data were collected, processed, and stored as 2D "planes." Figure 1 shows the locations of vertical electrode arrays (VEA), surface electrodes, and layouts of ERT planes for the Portsmouth Gaseous Diffusion Plant X701B Steam

Enhanced Extraction Pilot Study conducted in 1999 (LaBrecque, 2001). To collect a "plane" of data, a technician would connect a pair of VEA and several surface electrodes to the ERT system by plugging cables into a large panel of receptacles that looked a bit like that used by old-fashioned telephone operators. The operator would input the correct configuration information into the system and start the data collection process. A typical "plane" of data consisted of a pair of VEA, each with 15 electrodes, and 3 to 5 surface electrodes. Thus, each "plane" would contain roughly 1,000 data points and require about 10 minutes to collect. While one "plane" was being collected, the technician would transfer the data to a computer for processing and inversion. To present the data, a scientist would sort through the inverse results from the 40 planes and splice them together to create a pseudo 3-D presentation.

The primary advantage of the 2-D approach was that it made organization of the site, data collection, and data processing straightforward. Unfortunately, it has a number of shortcomings:

First, on-site labor is required. About 1.5 person-days of effort are required to complete the cycle from data collection to presentation. For long-term monitoring, the labor costs will typically exceed the costs of the monitoring system and the ERT electrode installation.

Second, 3-D imaging using 2-D data presents some problems. There is no assurance that a 2-D approach will give a realistic representation of 3-D structures. For example, we have encountered cases where strongly conductive structures such as pipes and well-casings produced resistive anomalies in 2-D images. One cannot circumvent this problem simply by applying a 3-D inversion routine to interpret 2-D data. There is simply not enough information to derive a correct, unique image.

Third, the 2-D data collection/handling strategy is not that efficient. In ERT surveys, it is important to collect all of the unique combinations of data including "common-borehole" data (where the transmitter and receiver electrodes are located within the same borehole). If each plane is collected and interpreted independently, then the same common-borehole data are collected several times per day. For example, Fig. 1 shows seven different planes that all use the VEA labeled 'N' (VEA-N). In this case, the common-borehole data for VEA-N were collected seven times during each field day. On average, the common-borehole data for a given well were collected four times per day. Removing this redundancy would cut the data collection time in half.

Finally, there are certain types of data that can be collected and interpreted only in 3-D. One such type of data uses horizontal dipoles with positive and negative transmitter and receiver electrodes all located in up to four different wells.

Three-Dimensional Autonomous Data Collection and Processing

In this section, we discuss two distinct, but very closely related concepts: first the advantages of collecting and processing data in a fully 3-D sense, that is collecting and interpreting data from groups of three or more VEA; and second the use of an autonomous system that collects and processes data without the need for human intervention.

Figure 2 shows a diagram of a layout of 3-D blocks for the same site shown in Fig. 1. The layout consists of 10 blocks each with 4 to 5 wells. The VEA locations at this site are not ideal for 3-D interpretation and some of the blocks overlap. We have also retained the original locations of the surface electrodes. If this site were laid out for 3-D interpretation, we would use slightly fewer, and more evenly distributed, surface electrodes, rather than placing them along the planes. With the increased flexibility inherent in a 3-D arrangement, we would collect a larger number of data points than was possible in the 2-D arrangements. By eliminating redundancies in the data collection, it is possible to collect twice as much data in about the same amount of time as the previous survey, about 6 hours. With a fully automated data system running continuously, a site four times this size could be collected overnight. To accomplish full 3-D data collection and interpretation, the data collection, processing, and inversion would need to be carefully planned and coordinated.

Ideally, we would like to connect the entire site to the measurement system at once. We would also like to have a fairly fast data acquisition rate; for a site with 200 electrodes we would have about 40,000 data points which would take about 12 hours to collect at 1 data point per second. The speed of data acquisition and the number of electrodes that can be connected to the multiplexer are inversely related. That is because the best way to speed up acquisition is to measure potentials at several receivers at the same time. The size, cost, and even the weight of a multiplexer are essentially proportional to the number of switch-points. Each switch-point allows one electrode to be hooked to either the plus or the minus terminal of either the transmitter or the receiver. Thus to connect a system with a transmitter, a single receiver channel, and 30 electrodes requires $4 \times 30 = 120$ switch-points. A multi-channel system with a transmitter, and three receiver channels for the same 30 electrodes requires 240 switch-points. Note that an alternative 240 switch-point system with a single receiver channel would allow connection to 60 electrodes. Thus, there is a tradeoff between the maximum number of electrodes, the speed of acquisition and the size and cost of the multiplexer.

It is also important to consider that doubling the number of receivers will not quite double the rate of data acquisition. This is because there is some overhead associated with controlling and communicating with multiple receivers. Also the data must be organized to allow

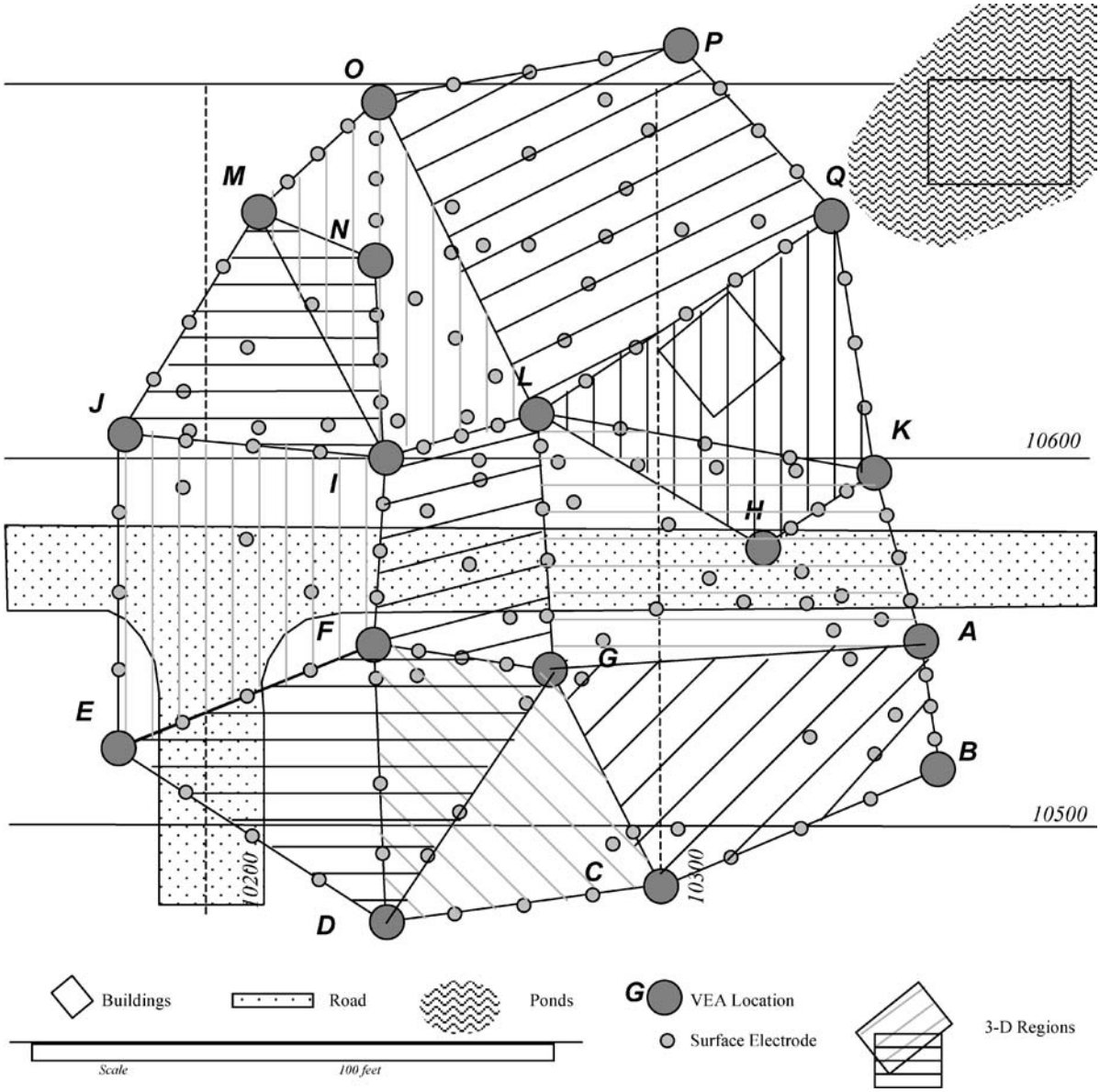

Figure 2. One possible layout of blocks for 3-D data collection and interpretation at the site shown in Fig. 1. Note that all of the blocks contain at least 4 electrodes and that some of the blocks overlap.

efficient use of multiple receivers. To use multiple channels efficiently, blocks of data that use the same transmitter electrodes but different receivers must be placed together.

Beyond cost, there are other problems with large multiplexers that have numerous switch-points. First, a great deal of time can be spent communicating with and controlling these systems. Second, even in a well-designed system, each switch point has a very large, but finite, electrical resistance and small, but significant, electrical capacitance. Both of these can allow tiny errors that tend to accumulate and may affect the measured response.

The goal therefore is to find ways to collect the most data in a given day with the smallest possible system with the minimum number of receiver channels. A fully autonomous system can help achieve this in two ways: first, we can collect data around the clock without the cost of multiple shifts of technicians to run the system, and second, we eliminate the time needed to manually switch and configure the system for each data run. For short, 5 to 10 minute, data runs, we find that roughly 25% of the time is spent either configuring the system or with the system idle waiting for the operator's input. For long, several-hour, data runs, the situation is often worse. Typically the operator leaves to work on other duties during the data run and the system may lie idle for hours waiting for him or her to return.

Data Processing

Pre-Inversion Processing

The quantity and complexity of 3-D data requires automated data processing as well as data collection. The form of the processing depends on data collection strategies, data interpretation strategies (2-D versus 3-D), and user needs in terms of turn-around time and the types of images used.

The processor needs to deal with the limitations of the data collection systems. For example, with older measurement systems, the arrays and multiplexer often used the same, local, arbitrary number system, for example 1 to 30, regardless of which wells were connected to the system. Somewhere in the processing sequence, the electrodes need to be translated to a global number system in terms of wells and electrodes or true Cartesian coordinates. This problem is avoided if the measurement system can be configured to use true coordinates or well and electrode numbers.

Typically pre-inversion processing of the data includes:

1) Input of one or more data files needed for an inversion of a 3-D region within the survey area;
2) Sort the data by electrode location and remove any data taken using electrodes that lie outside the inversion region;
3) Perform reciprocal (quality control) checks on the data, and throw out data with excessive errors and average the remaining data;
4) Locate and append the inversion control information to the field data to create an inversion input file;
5) Communicate with the inversion routine and let it know that the data are ready; and
6) Track the progress of the data collection system and inversion routines and move files that are no longer needed to a different folder or storage device for long-term storage and archiving.

Inversion Theory

As discussed earlier, the ERT method relies on sophisticated modeling algorithms. The work described in this paper used the 3-D anisotropic, Occam's inversion approach that was described by LaBrecque and Casale (2002). Occam's inversion seeks to find the smoothest possible solution that still fits the data within a specified a-priori value (LaBrecque *et al.,* 1999). An iterative approach is used in which a series of linear approximations are used to search for a solution to the nonlinear inverse problem. Each iteration starts by comparing the data with a forward solution, the numerical approximation of Equation (1):

$$\nabla \cdot \hat{\sigma} \nabla V = I, \tag{1}$$

where $\hat{\sigma}$ is conductivity, V is voltage, and I is current.

An anisotropic version of the finite-difference formulation of Dey and Morrison (1979) is used to solve for the potentials at a pair of receiver electrodes given within a 3-D anisotropic earth. This formulation uses the simplified form of anisotropy that assumes that the axes of the conductivity ellipse are aligned with the coordinate directions so that the conductivity tensor simplifies to

$$\hat{\sigma} = \begin{bmatrix} \sigma_{x,x} & 0 & 0 \\ 0 & \sigma_{y,y} & 0 \\ 0 & 0 & \sigma_{z,z} \end{bmatrix}. \tag{2}$$

A conjugate-gradient routine with a symmetric successive over-relaxation (SSOR) preconditioner is used to solve the linear system of equations for the forward problem (Spitzer, 1995).

The objective function, minimized using Occam's inversion, is given by

$$\boldsymbol{S}(\boldsymbol{m}) = (\boldsymbol{d}_{obs} - g(\boldsymbol{m}))^T \boldsymbol{W}_D (\boldsymbol{d}_{obs} - \boldsymbol{g}(\boldsymbol{m})) + \alpha\, \boldsymbol{m}^T\, \boldsymbol{R}\boldsymbol{m}, \tag{3}$$

where **d** is vector of data values, **m** is the vector of parameters, **g**(**m**) is the forward solution, $\mathbf{W}_D$ is the diagonal data weight matrix, **R** is the regularization operator which is discussed in detail below, $\mathbf{d}_{obs}$ is the vector of observed data, and α is an empirical factor that controls the amount of regularization versus the fit of the forward model to the data. Minimizing the objective function for large a value of α results in a smooth solution but a poor data fit. The optimal solution corresponds to the largest possible value of α which still fits the data to some a priori value. LaBrecque *et al*. (1999) discuss a method of iteratively determining α for 3-D inversion. In the new anisotropic algorithm, the parameters, **m**, are the natural logarithms of the three components of conductivity (X, Y, and Z) of each cell in the finite-difference mesh.

The nonlinear iterations can be expressed as

$$\mathbf{m}_{n+1} = \mathbf{m}_n + \Delta \mathbf{m}_n. \tag{4}$$

The parameter change vector at n^{th} iteration, $\Delta\mathbf{m}_n$, is obtained by solving the linear system

$$(\mathbf{G}_n{}^T \mathbf{W}_D \mathbf{G}_n + \alpha \mathbf{R}) \Delta \mathbf{m}_n = (\mathbf{G}_n{}^T \mathbf{W}_D (\mathbf{d}_{obs} - \mathbf{g}(\mathbf{m}_n)) - \alpha \mathbf{R} \mathbf{m}_n, \tag{5}$$

where the elements of the sensitivity matrix at iteration n, $\mathbf{G}_n$, are given by

$$\mathrm{G_n}^{ij} = \left. \frac{\partial g^i(\mathbf{m})}{\partial \mathrm{m}^j} \right|_{\mathbf{m}_n}, \tag{6}$$

and where $g^i(\mathbf{m})$ is the forward solution for the i^{th} data point and $\mathrm{G_n}^{ij}$ is the sensitivity at the n^{th} iteration of the i^{th} data point with respect to the j^{th} element.

The system of equations given by Equation (5) is positive-definite and is solved using the conjugate-gradient method with a diagonal preconditioner (LaBrecque *et al.,* 1999). A data-error reweighting scheme is implemented to suppress the effects of data outliers (Morelli and LaBrecque, 1996).

The choice of the regularization operator is critical to the success of the inverse algorithm. Three different regularization operators have been implemented in the anisotropic code. All three can be written in the general form:

$$\mathbf{R} = \mathbf{X}^{\mathbf{T}}\mathbf{X} + \mathbf{Y}^{\mathbf{T}}\mathbf{Y} + \mathbf{Z}^{\mathbf{T}}\mathbf{Z} + \mathbf{M}^{\mathbf{T}}\mathbf{M}, \qquad (7)$$

where $\mathbf{X}^{\mathbf{T}}\mathbf{X}$, $\mathbf{Y}^{\mathbf{T}}\mathbf{Y}$, and $\mathbf{Z}^{\mathbf{T}}\mathbf{Z}$ matrices are used to control the roughness in the X, Y and Z directions respectively and $\mathbf{M}^{\mathbf{T}}\mathbf{M}$ is used to minimize the anisotropy. The construction of the regularization operators are described in LaBrecque and Casale (2002).

Field Tests at the Vadose Zone Research Park

A Vadose Zone Research Park has been established at the INEEL to study water infiltration and the formation of perched-water lenses in a 150 meter thick, layered vadose zone. The Park is situated along the Big Lost River, which flows intermittently and has not flowed since June 2000. It hosts a pair of newly constructed percolation ponds (Street *et al.,* 2002). The first hydraulic testing of the ponds occurred in June 2002.

The goal of the project described below was to monitor the infiltration of water as the ponds were flooded. The Vadose Zone Research park is a good test bed for an autonomous data collection system for several reasons. First, the park has a relatively large spatial scale of about 2.25 hectares implying a need for a fair number of electrodes. Second, the location is fairly remote, about a one hour drive from Idaho Falls, Idaho; far enough that it was inconvenient for a person to check and operate the system. Third, the experiment occurred over a period of several weeks as the pumps and pipelines were tested; a period long enough that deployment of a dedicated operator would have been expensive and inefficient. Finally, at the time of the project, there was no direct communication to the site, no phone lines or internet connection.

The ERT system was installed prior to initial wetting to collect background data. It was then operated continuously and autonomously during the next few weeks while various infiltration events occurred as the ponds were tested. Although the site was not as complicated as those described above and not all of the features of an advanced autonomous system were implemented at the time of the study, the site served to test the basic concepts and to improve the overall system.

Prototype System Description

The prototype system was based on the MPT2002 ERT system built by Multi-Phase Technologies, LLC. For the initial tests the system had a single receiver-channel for monitoring voltage. The transmitter used a constant voltage supplied by an external power supply and a second receiver channel was used to measure the transmitted current.

The major reason for using a constant voltage source, rather than the constant-current source traditionally used for surface resistivity measurements, is that the electrode contact impedance can vary over orders of magnitude between different transmitting pairs within the ERT survey. Commonly, the uppermost electrodes are in shallow, dry, highly resistivity layers and the deepest are in electrically conductive zones below the water table. Systems that use a constant current source must determine the correct range of voltage and current that is compatible with the transmitter. This adds complexity to the measurement system and time to the measurements.

The receivers in the system are electrically isolated both from the system ground and from other receivers. Thus one of the receiver channels could be connected directly to a reference resistor on the transmitter and could still measure millivolt level signals. Resistivity and induced polarization (chargeability) were measured in the time domain. For this study, we used a 16.67 ms time window with a 20 millisecond delay for both the resistivity (transmitter on) and induced polarization (transmitter off) measurements. The window length was chosen to provide optimal rejection of power line noise. The resulting waveform has a primary frequency of approximately 6.5 Hz. At this frequency, it requires slightly more than 1 second to collect a single data point.

To remove self-potential and electrode noise the measurements were digitized using an analog to digital (A to D) converter rated by the manufacturer at 24 bits. In practice we found the true signal-to-noise ratio achieved by the A to D converter was about six decimal places (equivalent to 19–20 bits whereas 24 bit accuracy would imply 8 decimal places). Finally, a stacking routine designed to remove second-order polynomial trends in the data was applied.

The system has a multiplexer capable of transmitting and receiving on any combination of up to 60 electrodes. The receivers, transmitter, and multiplexers are all controlled by a Windows compatible field computer through a single serial port. For the prototype, we used a relatively simple method of automating the data acquisition. The existing operating software runs from an MS-Windows-based, menu-driven routine and interacts with a series of

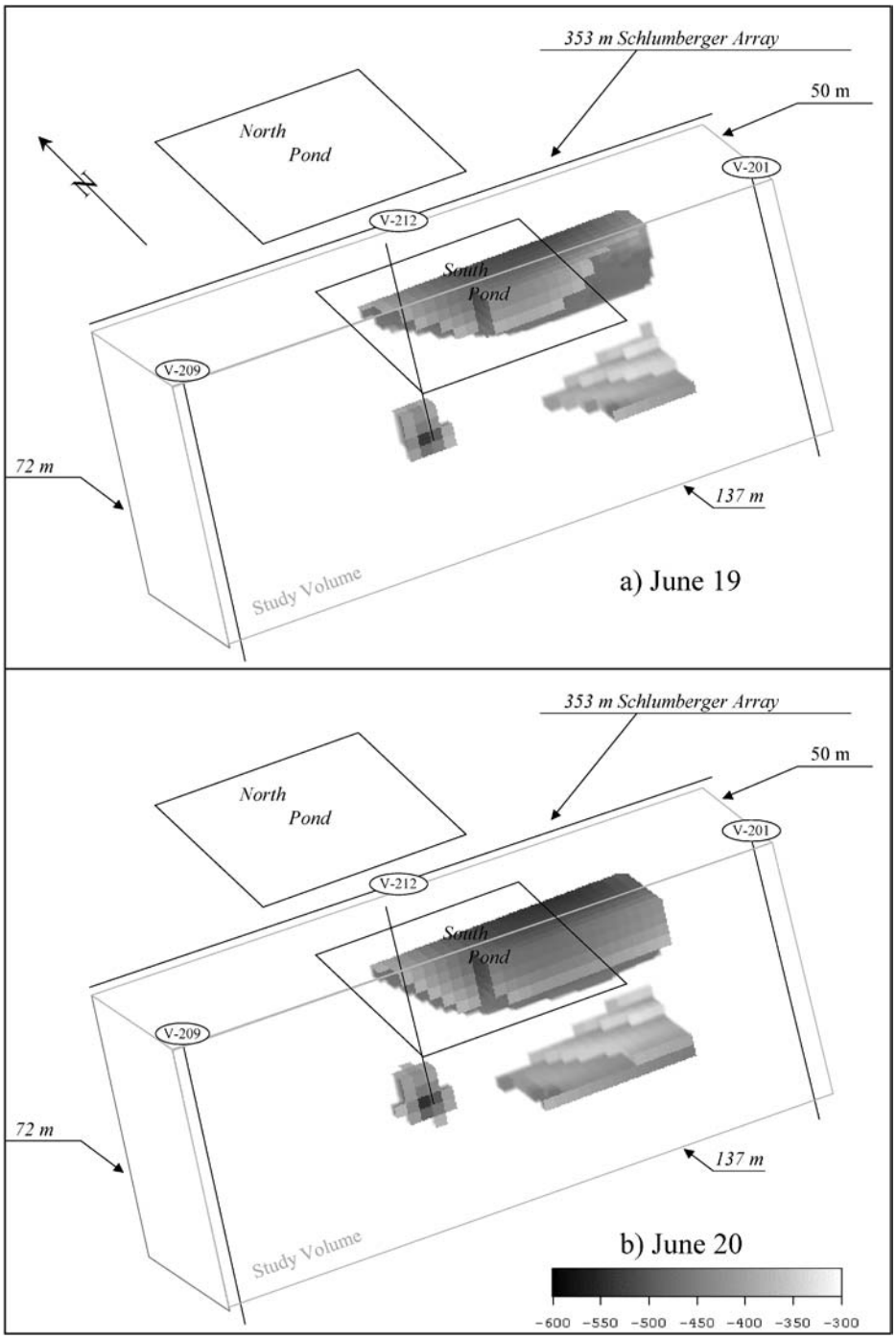

Figure 3. Three-D perspective view of resistivity changes during infiltration. Looking north-east. Resistivities shown are differenced from June 18 and are presented for a) June 19 and b) June 20. Values are ohm-m. Range is −300 to −600 ohm-m.

system configuration files. The configuration files were developed prior to installation at the site. Then the operating system was automated by using Quickeys® by CE Software Inc., a macro/scripting software for the Windows operating system, to start data acquisition at specific times using a specific configuration file.

Experiment Setup

The purpose of the project was to monitor infiltration on a pair of 61 m by 61 m ponds at the INEEL Vadose Zone Research Park. The two ponds are separated by approximately 15 m and one pond is directly north of the other. The

Table 1. Summary of infiltration schedule for the Vadose Zone Research Park.

Date(s)	Water added to north pond (m^3)	Water added to south pond (m^3)
June 18–19 2002	1020	3467
June 20, 2002	0	907
June 21, 2002	0	1927
June 24, 2002	0	1240
June 25, 2002	0	1158

ponds lie on top of about 4.5 m (15 ft) of alluvial sand and gravel that is underlain by interbedded basaltic lava flows and sediments. There are significant sediment interbeds at around 40 m and 60 m (Street *et al.,* 2002) within the basalt flows.

Prior to flooding the site, five electrode arrays were installed: three vertical electrode arrays (VEA) and two surface electrode arrays (Fig. 3). One VEA was centered between the ponds. The two surface arrays extend outward from this VEA along east-west lines between the ponds. Each surface array included thirty electrodes at 6-m intervals. The other VEA were located approximately 150 m apart in an east-west direction and 30 m south of the east-west line formed by the surface arrays. This positioned one VEA on each side of the south percolation pond, approximately 30 m distant from the pond, and at approximately 1/3 of the south extent of the pond. The depths of all three VEA were 70 m and electrodes were placed at 2.5 m intervals.

Various electrical data were available for collection. The significant data that were collected during each time period include Schlumberger sounding/profiling along the surface arrays, common-well and cross-well dipole-dipole data, and cross-well horizontal transmitters with vertical dipole receivers. We also collected pole-dipole-like data that used a vertical dipole in one VEA, a single electrode in a second well, and the bottom-most electrode in the third VEA as the reference electrode.

The data collection schedules included a pre-flood background dataset collected the morning of June 18, 2002. Subsequently data collection intervals were approximately every 5 hours. Continuous cycling over each 24 hour period resulted in 5–6 collection intervals per day. Each collection interval started and ended autonomously.

Results

Table 1 summarizes the amounts of water released into the two ponds. The initial release began on the afternoon of June 18th and continued overnight. The south pond was also flooded on June 21st, 24th, and 25th.

Background ERT data were collected the morning of June 18th. In Figs. 3 and 4, resistivity data are presented for midday June 19th, 20th, 21st and 24th. All of the data from a single time interval (usually a morning or afternoon) were combined and processed together for 3-D inversion. The images (Figs. 3 and 4) show resistivity differences, in ohm-meters, from the morning of June 18th.

In the first image (Fig. 3a), there is a large zone of decreased resistivity in the upper 15 m of the site, starting below the infiltration pond and extending somewhat eastward. This shows the increased saturation within the upper layer of sediments. There is also a pair of smaller, deeper, low-resistivity anomalies at the approximate depth of the inter-bedded sediment layer, around 40 m. The larger of these anomalies lies under the east side of the south pond. Within the basalt layers, the infiltrating water is moving through fractures which are smaller than the field configuration was able to image. It is also important to note that the configuration of the ERT arrays provides information only on the southern half of the site.

The subsequent images show the lateral expansion of the wetted zone within the sediments. The anomaly is largest for June 21st (Fig. 4c) and decreases somewhat by June 24th (Fig. 4d). This correlates well with the knowledge that no water was added to the system from June 21st until the morning of June 24th.

The pattern is more complex within the first interbedded sedimentary layer. The small anomaly near the western VEA shows little variation with time and remains localized near the VEA. One possible explanation is that leakage of a limited amount of water occurred down the borehole annulus. The larger, more tabular anomaly to the east appears to increase in size on June 20th (Fig. 3b), decrease somewhat on June 21st (Fig. 3c) and finally to increase substantially on June 24th (Fig. 3d).

Conclusions

There are substantial advantages to applying a fully 3-D, autonomous system to long-term monitoring. Although, at the time of the survey, we had not fully implemented all of the techniques possible with such a system, a prototype system successfully collected data using a variety of different arrays.

Data were collect over a two-week period essentially without an operator on the site. The data were used successfully to monitor the infiltration of water in the interbedded sediment and basalts at the INEEL Vadose Zone Research Park.

During operation, we found that there was a need to develop a more sophisticated operating system dedicated to autonomous operation. The existing system performs a number of self-monitoring operations. Using the menu-driven,

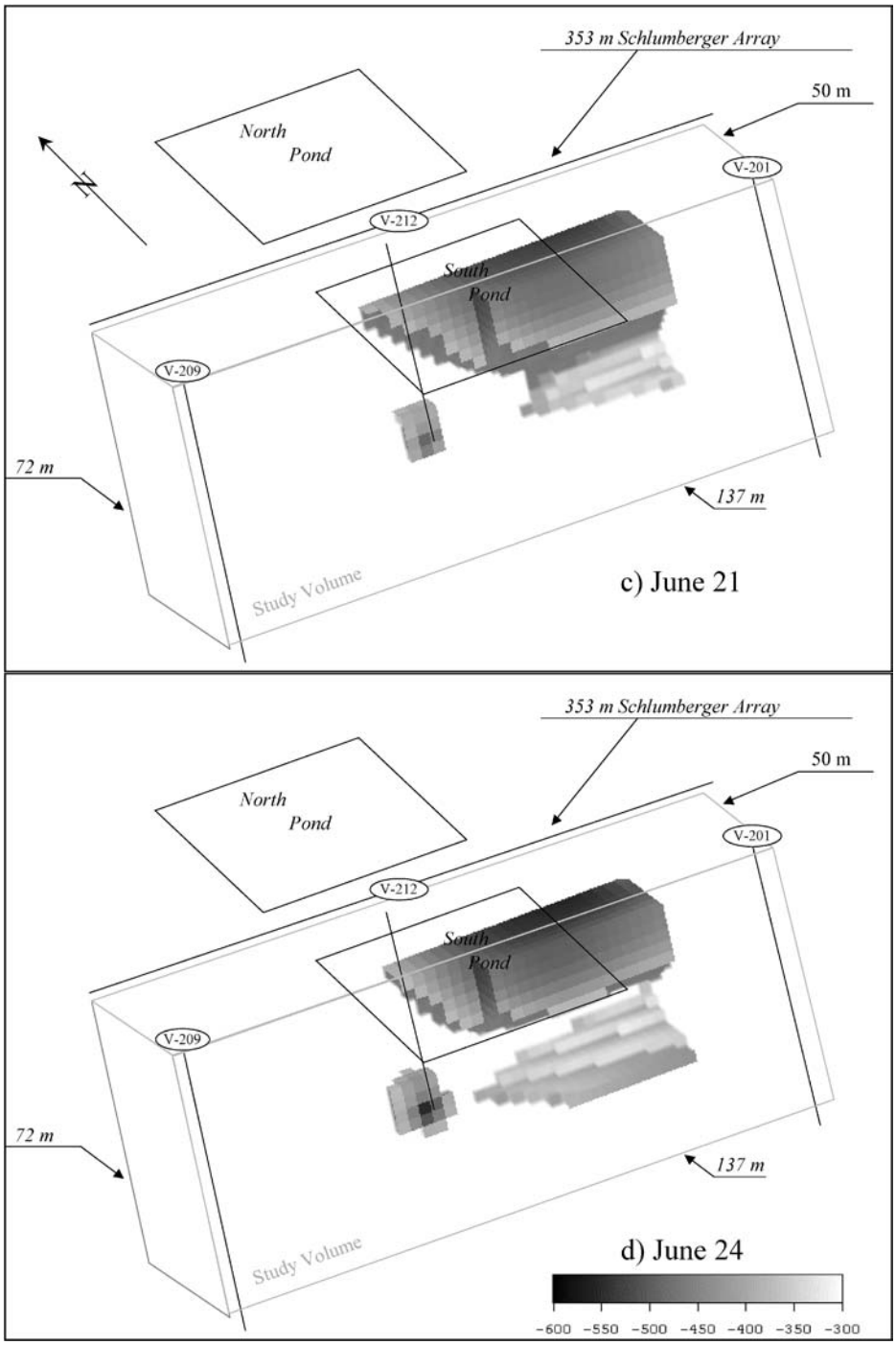

Figure 4. Continuation of Fig. 3 showing three-D perspective view of resistivity changes, differenced from Jun 18 for c) June 21 and d) June 24. Resistivity values are in ohm-m and the range of values displayed is −300 to −600 ohm-m.

operator-oriented operating system, the data collection system was designed to halt operation and inform the operator of any system problems. In the field trial, we compensated for this by collecting multiple data sets, thus assuring that one or more complete data sets were collected during each day of operation. Our experience using this method suggests that, in autonomous systems, the system needs to be able to continue operations rather than halt for any situation that does not threaten to damage the system even in cases where only part of the data may be collected. Ideally, such a system should be able to adapt to problems and if necessary contact the operators remotely when problems occur.

Acknowledgments

The work presented above was supported through the INEEL Laboratory Directed Research & Development Program under DOE Idaho Operations Office Contract DE-AC07-99ID13727.

References

Daily, W.D., Ramirez, A., LaBrecque, D.J., and Nitao, J., 1992, Electrical resistivity tomography of vadose water movement: Water Resources Research, **28**, 1429–1442.

Daily, W., and Ramirez, A., 1999, Electrical imaging of engineered hydraulic barriers: Proceedings of the Symposium on the Application of Geophysics for Environmental and Engineering Problems (SAGEEP) '99, 683–692.

Dey, A., and Morrison, H.F., 1979, Resistivity modeling for arbitrarily shaped three-dimensional structures: Geophysics, **44**, 753–780.

LaBrecque, D.J., 2001, The role of advanced monitoring in steam stripping for in situ remediation of DNAPL: Proceedings of the Symposium on the Application of Geophysics for Environmental and Engineering Problems (SAGEEP) '01, compact disk paper OSC-4, 14 pp.

LaBrecque, D., Bennett, J., Heath, G., Schima, S., and Sowers, H., 1998, Electrical resistivity tomography monitoring for process control in environmental remediation: Proceedings of the Symposium on the Application of Geophysics for Environmental and Engineering Problems (SAGEEP) '98, 613–622.

LaBrecque, D.J., and Casale, D., 2002, Experience with anisotropic inversion for electrical resistivity tomography: Proceedings of the Symposium on the Application of Geophysics to Engineering and Environmental Problems (SAGEEP) '02, compact disk paper 11ELE7, 10 pp.

LaBrecque, D.J., Miletto, M., Daily, W., Ramirez, A., and Owen, E., 1996a, The effects of noise on Occam's inversion of resistivity tomography data: Geophysics, **61**, 538–548.

LaBrecque, D.J., Ramirez, A.L., Daily, W.D., Binley, A.M., and Schima, S.A., 1996b, ERT monitoring of environmental remediation processes: Measurement Science and Technology, **7**, 375–383.

LaBrecque, D.J., Morelli, G., Daily, W., Ramirez, A., and Lundegard, P., 1999, Occam's Inversion of 3D ERT data: *in* Three-dimensional electromagnetics, Spies, B. (ed.), Soc. of Expl. Geophys., Tulsa, 575–590.

LaBrecque, D.J., Morelli, G., and Lundegard, P.D., 1997, Effective electrical resistivity tomography surveys for environmental monitoring: Proceedings of the Symposium on the Application of Geophysics to Engineering and Environmental Problems (SAGEEP) '97, 881–887.

LaBrecque, Douglas, J., and Yang, Xianjin, 2001, Difference inversion of ERT data: A fast inversion method for 3-D in situ monitoring: Journal of Environmental and Engineering Geophysics, **6**, 83–90.

Lundegard, P.D., and LaBrecque, D.J., 1995, Air sparging in a sandy aquifer (Florence Oregon): Actual and apparent radius of influence: Journal of Contaminant Hydrology, **19**, 1–27.

Lundegard, P.D., and LaBrecque, D.J., 1998, Geophysical and hydrological monitoring of air sparging flow behavior: Comparison of two extreme sites: Remediation, Summer 1998, 59–72.

Morelli, G., and LaBrecque, D.J., 1996, Robust scheme for ERT inverse modeling: European Journal of Environmental and Engineering Geophysics, **2**, 1–14.

Ramirez, A., Daily, W., LaBrecque, D., Owen, E., and Chesnut, D., 1993, Monitoring an underground steam injection process using electrical resistance tomography: Water Resources Research, **29**, 73–87.

Ramirez, A.L., Daily, W.D., and Newmark, R.L., 1995, Electrical resistance tomography for steam injection monitoring and process control: Journal of Environmental and Engineering Geophysics, **0**, 39–52.

Sasaki, Y., 1992, Resolution of resistivity tomography inferred from numerical simulation: Geophys. Prosp., **40**, 453–464.

Sasaki, Y., 1994, 3-D resistivity inversion using the finite-element method: Geophysics, **59**, 1839–1848.

Schima, S.A., LaBrecque, D.J., and Miletto, M., 1993, Tracking fluid flow in the unsaturated zone using cross-borehole resistivity and IP: Proceedings of the Symposium on the Application of Geophysics to Engineering and Environmental Problems (SAGEEP) '93, 527–544.

Schima, S., LaBrecque, D.J., and Lundegard, P.D., 1996, Using resistivity tomography to monitor air sparging: Ground Water Monitoring and Remediation, **16**, 131–138.

Shima, Hiromasa, and Sakayama, T., 1987, Resistivity tomography: An approach to 2-D resistivity inverse problems: 57th Annual Internat. Mtg., Soc. Expl. Geophys., Expanded Abstracts, Session:EM1. 4.

Shima, H., 1990, Two-dimensional automatic resistivity inversion technique using alpha centers: Geophysics, **55**, 682–694.

Spitzer, K., 1995, A 3-D finite difference algorithm for DC resistivity modeling using conjugate gradient methods: Geophysical J. Int'l, **123**, 903–914.

Street, L., Bishop, C., and Hull, L., 2002, Baseline Moisture Monitoring at the INEEL Vadose Zone Research Park: Proceedings of the American Nuclear Society Spectrum 2002 Meeting, on compact disk, paper 54301, 7 pp.

Zhang, J., Mackie, R.L., and Madden, T.R., 1995, 3-D resistivity forward modeling using conjugate gradients: Geophysics, **60**, 1313–1325.